This is a preprint of: "Global dynamics of a virus model with invariant algebraic surfaces", Fabio Scalco Dias, Jaume Llibre, Clàudia Valls, *Rend. Circ. Mat. Palermo (2)*, 2019.
DOI: [10.1007/s12215-019-00417-0]

GLOBAL DYNAMICS OF A VIRUS MODEL WITH INVARIANT ALGEBRAIC SURFACES

FABIO SCALCO DIAS[1], JAUME LLIBRE[2] AND CLAUDIA VALLS[3]

ABSTRACT. In this paper by using the Poincaré compactification in $\mathbb{R}^3$ we make a global analysis for the virus system

$$\dot{x} = \lambda - dx - \beta xz, \quad \dot{y} = -ay + \beta xz \quad \dot{z} = ky - \mu z$$

with $(x, y, z) \in \mathbb{R}^3$, $\beta > 0$, λ, a, d, k and μ are nonnegative parameters due to their biological meaning. We give the complete description of its dynamics on the sphere at infinity. For two sets of the parameter values the system has invariant algebraic surfaces. For these two sets we provide the global phase portraits of the virus system in the Poincaré ball (i.e. in the compactification of $\mathbb{R}^3$ with the sphere $\mathbb{S}^2$ of the infinity).

1. INTRODUCTION AND STATEMENT OF THE MAIN RESULTS

In this work we do a global analysis of the virus system

$$\begin{aligned} \dot{x} &= P(x, y, z) = \lambda - dx - \beta xz, \\ \dot{y} &= Q(x, y, z) = -ay + \beta xz, \\ \dot{z} &= R(x, y, z) = ky - \mu z, \end{aligned} \tag{1}$$

where the state variables are $(x, y, z) \in \mathbb{R}^3$, $\beta > 0$, λ, a, d, k and μ are nonnegative parameters due to their biological meaning. As usual, the dots denote derivative with respect to the time t. Note that β cannot be zero otherwise the differential system becomes linear, and consequently its study is trivial. System (1) was proposed in the book [7]. For more studies related with virus models, including the importance of our model (1), we refer the readers to [5, 8].

Let $\mathbb{R}[x, y, z]$ be the ring of real polynomials in the variables the variables x, y and z. We say that $F = F(x, y, z) \in \mathbb{R}[x, y, z]$ is a *Darboux polynomial* of system (1) if it satisfies $(\nabla F) \cdot (P, Q, R) = KF$, where $K = K(x, y, z)$ is a real polynomial of degree at most 1, called the *cofactor* of $F(x, y, z)$. If the cofactor is zero, then $F(x, y, z)$ is a

2010 *Mathematics Subject Classification.* 34A34, 34C05, 34C14 .
Key words and phrases. Invariant algebraic surfaces, Poincaré compactification, phase portrait, dynamics at infinity, virus model.

polynomial first integral of system (1). If $F(x,y,z)$ is a Darboux polynomial, then the algebraic surface $F(x,y,z)=0$ is called an *invariant algebraic surface*; i.e. if an orbit of system (1) has a point on this surface, then the whole orbit is contained in it.

We say that a C^1 function $I(x,y,z,t)$ is an *invariant* of the differential system (1) if $dI/dt=0$ on the trajectories of the system. When an invariant function is independent of the time t, then it is a *first integral*. When a system has a Darboux polynomial F with a constant factor $k=k_0\in\mathbb{R}$, then the function $I(x,y,z,t)=F(x,y,z)e^{-k_0t}$ is called a *Darboux invariant* of that system, see Chapter 8 of [3].

We say that the Darboux polynomials $F_1,\ldots,F_n$ *generate* all the Darboux polynomials of system (1) if any Darboux polynomial F of system (1) can be written as $F=F_1^{\alpha_1}\cdots F_n^{\alpha_n}$ with $\alpha_k\in\mathbb{N}$ for $k=1,\ldots,n$.

The following theorem proved in [9] summarizes the results on the existence of invariant algebraic surfaces for system (1).

Theorem 1. *When $\beta k(\lambda^2+d^2)\neq 0$, a set of generators for the set of all Darboux polynomials of system (1) are given in Table 1.*

Darboux Polynomial	Cofactor	Parameters
$F_0=x$,	$K=-d-\beta z$,	$\lambda=0$,
$F_1=x+y-\lambda/d$,	$K=-d$,	$a=d\neq 0$,
$F_2=x+y+(a-d)z/k-\lambda/d$,	$K=-d$,	$\mu=d\neq 0$.

TABLE 1. Invariant algebraic surfaces of system (1).

As any polynomial differential system the virus system (1) can be extended to an analytic system on a closed ball of radius one, whose interior is diffeomorphic to $\mathbb{R}^3$ and its boundary, the 2–dimensional sphere $\mathbb{S}^2$, plays the role of the infinity because in $\mathbb{R}^3$ one can go or come from infinity in as many directions as points have $\mathbb{S}^2$. This closed ball is denoted by B and called the *Poincaré ball*. The technique for doing such an extension is precisely the Poincaré compactification for a polynomial differential system in $\mathbb{R}^3$, which is described in details in [2], see also [1]. By using this compactification technique the dynamics of system (1) at infinity can be determined.

Theorem 2. *The phase portrait of the Poincaré compactification of system (1) at the infinity $\mathbb{S}^2$ is topologically equivalent to the one described in Figure 1.*

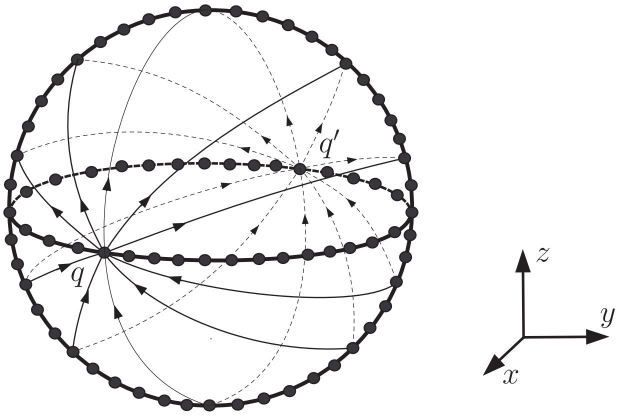

FIGURE 1. Phase portrait of the virus system (1) at the infinity $\mathbb{S}^2$ of the Poincaré ball. The circles of $\mathbb{S}^2$ contained in $x = 0$ and $z = 0$ are filled of singular points. Additionally there are two diammetrally opposite singular points on $z = 0$ of nodal type.

We go further and describe the global dynamics of system (1) for fixed values of the parameters having the invariant planes $F_1 = 0$ or $F_2 = 0$ described in Table 1.

Theorem 3. *The following statements hold for system (1) when* $\beta k(\lambda^2 + d^2) \neq 0$.

(a) *For* $d = a \neq 0$ *system (1) has the Darboux polynomial*

$$F_1(x, y, z) = x + y - \lambda/d$$

and the Darboux invariant

$$I_d(x, y, z, t) = (x + y - \lambda/d)e^{dt}.$$

The singular points on $F_1(x, y, z) = 0$ *are described in Table* 2. *The phase portraits of system (1) restricted to the compactified invariant plane* $F_1(x, y, z) = 0$ *are described in Figure 7.*

(b) *For* $d = \mu \neq 0$ *system (1) has the Darboux polynomial*

$$F_2(x, y, z) = x + y + \frac{(a - d)}{k}z - \frac{\lambda}{d}$$

and the Darboux invariant

$$I_d(x, y, z, t) = \left(x + y + \frac{(a - d)}{k}z - \frac{\lambda}{d}\right)e^{dt}.$$

The singular points on $F_2(x, y, z) = 0$ *are described in Table* 2. *The phase portraits of system (1) restricted to the compactified invariant plane* $F_2(x, y, z) = 0$ *are described in Figure 7.*

We remark that system (1) restricted to the invariant plane $F_0 = x = 0$ with $\lambda = 0$ is linear.

We say that a set $V \subset B$ is *invariant* by the flow of system (1) if for any $p \in V$ the whole orbit passing through p is contained in V. The sphere of the infinity always is an invariant set. Let $\varphi(t) = \varphi(t, p)$ be the solution of the compactified system (1) passing through the point $p \in B$ when $t = 0$, defined on its maximal interval $I_p = \mathbb{R}$ (because B is compact). Then the *α–limit set* of φ is the invariant set

$$\alpha(\varphi) = \{q \in B : \exists \{t_n\} \text{ such that } t_n \to -\infty \text{ and } \varphi(t_n) \to q \text{ as } n \to \infty\}.$$

In a similar way the *ω–limit set* of φ is the invariant set

$$\omega(\varphi) = \{q \in B : \exists \{t_n\} \text{ such that } t_n \to \infty \text{ and } \varphi(t_n) \to q \text{ as } n \to \infty\}.$$

The following theorem gives a complete description of the α– and ω–limit sets in the Poincaré ball, including its boundary $\mathbb{S}^2$, for system (1) having the invariant algebraic surfaces of Table 1.

Theorem 4. *Let γ be an orbit of the compactified system (1) with $\beta k \neq 0$. Assume $a = d \neq 0$, or $\mu = d \neq 0$. If γ is contained in the interior of B and outside the invariant plane $F_1 = 0$ if $a = d \neq 0$, or $F_2 = 0$ if $\mu = d \neq 0$, then the following two statements hold.*

(a) *The α–limit set of γ is some of the four infinite singular points q, q', E_2, E_2' contained in the boundary of the plane $F_i = 0$ for $i = 1, 2$.*

(b) *The ω–limit set of γ is contained in the closure of the invariant plane $F_i = 0$ in the Poincaré ball. More precisely,*
If $\mu = \lambda = 0$, or $\lambda = a = 0$, then $\omega(\gamma) \subset \overline{\{(0, 0, z), z \in \mathbb{R}\}}$, i.e. the straight line $x = 0$ of Figure 7.

If $\mu = 0$ and $\lambda \neq 0$, or $a = 0$ and $\lambda \neq 0$, then $\omega(\gamma) \subset \{P_0, E_2, E_2'\}$.

If $\mu \neq 0$ and $\beta k\lambda = d^2\mu$, or $a \neq 0$ and $\beta k\lambda = ad^2$, then $\omega(\gamma) = \{P_0\}$.

If $\mu \neq 0$ and $\beta k\lambda \neq d^2\mu$, or $a \neq 0$ and $\beta k\lambda \neq ad^2$, then $\omega(\gamma) \subset \{P_0, P_1\}$.

Here P_0, P_1 are singular points of system (1), contained in the plane $F_1 = 0$ (see Table 2), E_2 is the origin of the local chart U_2, $q = (-1, 0, 0)$ is a singular point in the local chart U_1, and E_2' and q' are the diametrally opposite points to E_2 and q in the Poincaré sphere.

The paper is organized as follows. In section 2 we prove Theorem 2 by using the Poincaré compactification for a polynomial vector field in $\mathbb{R}^3$. In section 3 we prove Theorem 3 by using the Poincaré compactification for a polynomial vector field in $\mathbb{R}^2$. For precise definitions of all these notions see Chapter 5 of [3]. Finally the proof of Theorem 4 is given in section 4.

2. Proof of Theorem 2

In this section we analyze the flow of system (1) at infinity. Consider system (1) or equivalently its associated polynomial vector field $X = (\lambda - dx - \beta xz, -ay + \beta xz, ky - \mu z)$.

In the next three subsections we will study the Poincaré compactification, $p(X)$, of system (1) in the local charts U_i and V_i, $i = 1, 2, 3$ in order to understand the global behavior of the solutions near infinity. See [1] for more details on these charts.

2.1. In the local chart U_3.

Using the results of [1] we have that the expression of the Poincaré compactification $Z_3 = p(X)$ of system (1) in the local chart U_3 is given by

$$\begin{aligned} \dot{z}_1 &= -\beta z_1 + z_3((\mu - d)z_1 + \lambda z_3 - k z_1 z_2), \\ \dot{z}_2 &= \beta z_1 + z_3((\mu - a)z_2 - k z_2^2), \\ \dot{z}_3 &= -z_3^2(k z_2 - \mu). \end{aligned} \tag{2}$$

In the points of the sphere $\mathbb{S}^2$ that correspond to the points at infinity we have $z_3 = 0$, and so system (2) becomes

$$\dot{z}_1 = -\beta z_1, \quad \dot{z}_2 = \beta z_1, \quad \dot{z}_3 = 0.$$

After eliminating the common factor z_1 (by rescaling of the time) we do not obtain any singular point in the local chart U_3 which is distinguished. From this system we see that system (2) has at infinity a continuum of singular points given by $(0, z_2, 0)$. Moreover $DZ_3(0, z_2, 0)$ has, for each z_2, the eigenvalues $-\beta$ and 0 with multiplicity 2. By the normal hyperbolicity theory (see [4] for details) to each point $(0, z_2, 0)$ it arrives two orbits, see Figure 2. Note that the equilibria $(0, z_2, 0)$ with $z_2 \in \mathbb{R}$ represent half of a great circle through the north pole of $\mathbb{S}^2$. The orbits of the system in the local chart U_3 at infinity have the phase portrait given in Figures 2 and 1.

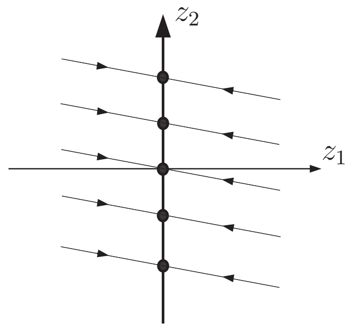

FIGURE 2. The phase portrait in the local chart U_3 at infinity.

2.2. **In the local chart U_1.** In the same way the Poincaré compactification $Z_1 = p(X)$ of system (1) in the local chart U_1 is

$$
\begin{aligned}
\dot{z}_1 &= \beta z_2(z_1+1) + z_3((d-a)z_1 - \lambda z_1 z_3),\\
\dot{z}_2 &= \beta z_2^2 + z_3((d-\mu)z_2 + kz_1 - \lambda z_2 z_3),\\
\dot{z}_3 &= z_3(dz_3 + \beta z_2 - \lambda z_3^2).
\end{aligned} \tag{3}
$$

System (3) restricted to infinity (that is with $z_3 = 0$) becomes

$$\dot{z}_1 = \beta z_2(z_1+1), \quad \dot{z}_2 = \beta z_2^2, \quad \dot{z}_3 = 0.$$

So there is a line of singular points which is $z_2 = 0$. These singular points are such that $DZ_1(z_1, 0, 0)$ has, for each z_1 the eigenvalue 0 with multiplicity 3. After eliminating the common factor z_2 (by a rescaling of the time) we get that the unique singular point is $q = (-1, 0, 0)$ which is an unstable node. Note that the equilibria $(z_1, 0, 0)$ for $z_1 \in \mathbb{R}$ represent in the Poincaré sphere $\mathbb{S}^2$ half of the equator. The orbits of the system in the local chart U_1 at infinity have the phase portrait given in Figures 3 and 1.

2.3. **In the local chart U_2.** The expression of the Poincaré compactification $Z_2 = p(X)$ in the local chart U_2 is

$$
\begin{aligned}
\dot{z}_1 &= -\beta z_1 z_2(z_1+1) + z_3((a-d)z_1 + \lambda z_3),\\
\dot{z}_2 &= -\beta z_1 z_2^2 + z_3(k + (a-\mu)z_2),\\
\dot{z}_3 &= z_3(az_3 - \beta z_1 z_2).
\end{aligned} \tag{4}
$$

Now the unique point of the local chart U_2 which is not covered by the local charts U_1, V_1, U_3 and V_3 is the origin of coordinates of U_2. System (4) restricted at the infinity (that is with $z_3 = 0$) becomes

$$\dot{z}_1 = -\beta z_1 z_2(z_1+1), \quad \dot{z}_2 = -\beta z_1 z_2^2, \quad \dot{z}_3 = 0.$$

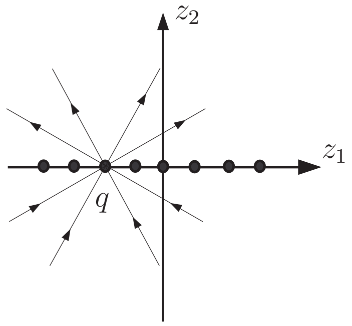

FIGURE 3. The phase portrait in the local chart U_1 at infinity.

There are two lines of singular points $z_1 = 0$ and $z_2 = 0$. After removing these two lines of singular points, there is a singular point $q = (-1, 0, 0)$ which is a stable node and its local phase portrait is the one given in Figure 4.

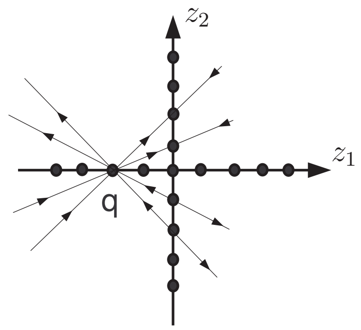

FIGURE 4. Local phase portrait at the origin of U_2 at infinity.

We observe that the flows in the V_i charts for $i = 1, 2, 3$ are the same as the ones in the respective U_i charts for $i = 1, 2, 3$ but with the time reversed because the compactified vector field $p(X)$ in V_i coincides with the vector field in U_i multiplied by -1 for each $i = 1, 2, 3$. See [1].

From subsections 2.1, 2.2 and 2.3 it follows the proof of Theorem 2.

3. Proof of Theorem 3

In Theorem 1 it was proved that the virus system (1) has the invariant algebraic surfaces $F_1(x, y, z) = x + y - \lambda/d = 0$ when $a = d \neq 0$

and $F_2 = x + y + (a-d)z/k - \lambda/d = 0$ when $\mu = d \neq 0$. It is easy to see that $I_d(x,y,z,t) = F_i(x,y,z)e^{dt}$ satisfies

$$\frac{dI_d}{dt} = \frac{\partial I_d}{\partial t} + \frac{\partial I_d}{\partial x}\dot{x} + \frac{\partial I_d}{\partial y}\dot{y} + \frac{\partial I_d}{\partial z}\dot{z} = e^{dt}\left(F_i(x,y,z)d + \frac{dF_i}{dt}\right) = 0,$$

where $i = \{1,2\}$. Therefore I_d is a Darboux invariant of system (1). This completes the proof of the first part of statements (a) and (b) of Theorem 3.

System (1) has two isolated singular points in $\mathbb{R}^3$, namely

$$p_0 = \left(\frac{\lambda}{d}, 0, 0\right), \quad p_1 = \left(\frac{a\mu}{\beta k}, \frac{\lambda}{a} - \frac{d\mu}{\beta k}, \frac{\lambda k}{a\mu} - \frac{d}{\beta}\right). \tag{5}$$

Note that these two singular points are on the two invariant algebraic surfaces $F_1(x,y,z) = 0$ when $a = d \neq 0$ and $F_2(x,y,z) = 0$ when $\mu = d \neq 0$. In what follows we shall analyze the flow of the system in these planes and relate their dynamics with the dynamics at infinity.

3.1. **Phase portrait on $\{F_1(x,y,z) = 0\}$.** We can consider in this subsection system (1) with $a = d \neq 0$ and $\beta k d(\lambda^2 + d^2) \neq 0$. System (1) restricted to the invariant plane $F_1(x,y,z) = 0$ is given by the differential system

$$\dot{x} = \lambda - dx - \beta xz, \quad \dot{z} = -kx - \mu z + \frac{k\lambda}{d}. \tag{6}$$

Doing the change of variables (with a rescaling of time)

$$x = \frac{d^2}{\beta k}X + \frac{\lambda}{d}, \quad z = \frac{d}{\beta}Z, \quad t = dT, \tag{7}$$

system (6) becomes

$$\dot{x} = -x - a_1 z - xz, \quad \dot{z} = -x - a_2 z \tag{8}$$

where $a_1 = \beta k\lambda/d^3, a_2 = \mu/d \in [0,\infty)$, and we have renamed the new variables (X,Z) by (x,z), and the dot denotes derivative with respect to the new time T.

We now study the infinite singular points of system (8). We will use the Poincaré compactification for a polynomial vector field in $\mathbb{R}^2$ which is described in Chapter 5 of [3].

3.1.1. *Infinite singular points.* System (8) in the local chart U_1 becomes

$$\dot{z}_1 = -z_2 + z_1(z_1 + (1-a_2)z_2 + a_1 z_1 z_2), \quad \dot{z}_2 = z_2(z_1 + z_2 + a_1 z_1 z_2).$$

When $z_2 = 0$ the only infinite singular point is the origin. Since the origin is nilpotent, using Theorem 3.5 of [3] we obtain that the phase portrait of the origin consists of one hyperbolic, one elliptic and two parabolic sectors, see Figure 5.

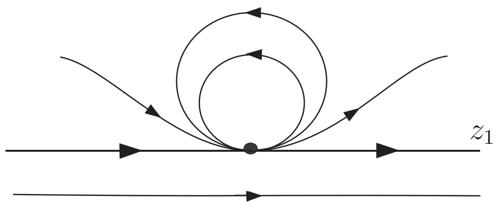

FIGURE 5. Local phase portrait at the origin of U_1 at infinity.

Now it only remains to study if the point $(0,0)$ of the local chart U_2 is a singular point. System (8) in the local chart U_2 writes

$$(9) \qquad \dot{z}_1 = -z_1 + z_2(-a_1 + (a_2-1)z_1 + z_1^2), \quad \dot{z}_2 = z_2^2(a_2 + z_1).$$

By a linear change of coordinates this system can be written as

$$\dot{z}_1 = -a_2 z_1^2 + a_1 z_1^3 - z_1^2 z_2, \quad \dot{z}_2 = z_2 - a_1 z_1^2 + (1-a_2) z_1 z_2 + a_1 z_1^2 z_2 - z_1 z_2^2.$$

Therefore $(0,0)$ is a semi–hyperbolic point. By Theorem 2.19 of [3] if $a_2 \neq 0$ we have that $(0,0)$ is a saddle–node point and going back to system (9) its local phase portrait is the one described in Figure 6.

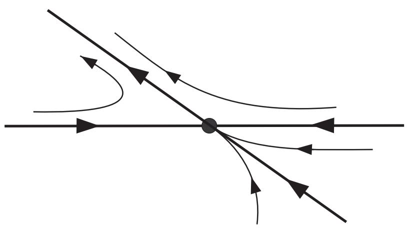

FIGURE 6. Local phase portrait at the origin of U_2 at infinity.

On the other hand, if $a_2 = 0$ but $a_1 \neq 0$, $(0,0)$ is a stable topological node. Finally, when $a_2 = a_1 = 0$, the system becomes

$$\dot{z}_1 = -z_1^2 z_2, \quad \dot{z}_2 = z_2(1 + z_1 - z_1 z_2),$$

so there is a line of singular points which is $z_2 = 0$. After eliminating the common factor z_2 (by a rescaling of the time) we do not obtain any singular point in the local chart U_2 which is distinguished.

3.1.2. *Finite singular points.* In what follows we shall study the local stability at the singular points of system (8) for the parameters a_1 and a_2.

Case 1: $a_2 = 0$. In this case system (8) becomes

$$\dot{x} = -x - a_1 z - xz, \quad \dot{z} = -x.$$

When $a_1 = 0$ the system has a continuum of singular points $(0, z)$ on the straight line $x = 0$. When $a_1 \neq 0$, the unique singular point is $(0, 0)$. The eigenvalues are

$$\lambda_1 = \frac{-1 + \sqrt{1 + 4a_1}}{2} \quad \text{and} \quad \lambda_2 = \frac{-1 - \sqrt{1 + 4a_1}}{2}.$$

As $a_1 > 0$, the origin is a saddle.

Case 2: $a_2 \neq 0$. In this case system (8) has exactly the two finite singular points:

$$P_0 = (0, 0), \quad \text{and} \quad P_1 = \left(a_2 - a_1, \frac{a_1 - a_2}{a_2}\right).$$

The eigenvalues of the linear part at these singular points are

$$\frac{-(a_2 + 1) \pm \sqrt{(a_2 + 1)^2 + 4(a_1 - a_2)}}{2} \quad \text{for} \quad P_0, \quad \text{and}$$

$$\frac{-(a_1 + a_2^2) \pm \sqrt{(a_1 + a_2^2)^2 + 4a_2^2(a_2 - a_1)}}{2} \quad \text{for} \quad P_1.$$

When $a_2 < a_1$, P_0 is a saddle and P_1 is an attractor node. On the other hand, when $a_1 < a_2$, P_0 is an attractor node and P_1 is a saddle. Finally, when $a_1 = a_2$, we have that $P_0 = P_1$. It is semi-hyperbolic and using Theorem 2.19 of [3] we conclude that it is a saddle-node. In short we have Table 2.

Parameters	Finite singular points	Figures
$a_1 = a_2 = 0$	line $x = 0$	Figure 7 (a)
$a_2 = 0, a_1 > 0$	P_0 saddle	Figure 7 (b)
$a_2 > 0, a_1 = a_2$	$P_0 = P_1$ saddle–node	Figure 7 (c)
$a_2 > 0, a_1 < a_2$	P_0 stable node, P_1 saddle	Figure 7 (d)
$a_2 > 0, a_1 > a_2$	P_0 saddle , P_1 stable node	Figure 7 (d)

TABLE 2. Finite singular points for the differential system (8) and for the parameters $a_1 = \beta k \lambda / d^3$ and $a_2 = \mu / d$ if $a = d \neq 0$, and $a_1 = \beta k \lambda / d^3$ and $a_2 = a/d$ if $\mu = d \neq 0$.

Taking into account the local information on the finite and infinite singular points of system (8) we get that the global phase portraits of systems (8) are topologically equivalent to those described in the Figure 7.

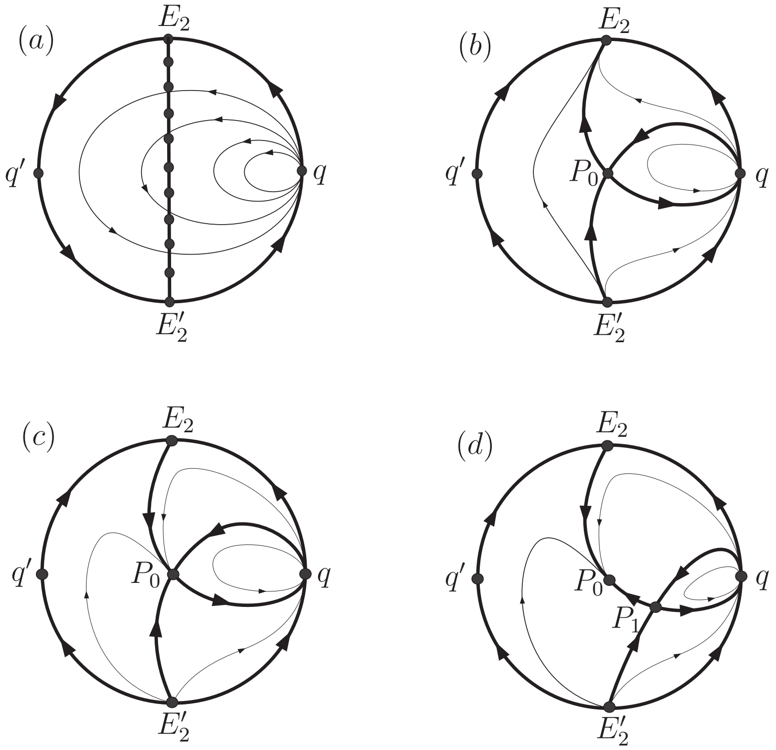

FIGURE 7. Phase portrait in the Poincaré disc of the virus system (1) on the invariant planes $F_1 = x + y - \lambda/d = 0$ if $a = d \neq 0$.

3.2. **Phase portrait on** $F_2(x, y, z) = 0$**.** In this subsection we consider system (1) with $\mu = d \neq 0$ and $\beta k d \neq 0$. System (1) restricted to the invariant plane $F_2(x, y, z) = 0$ is given by the differential system

$$\dot{x} = \lambda - dx - \beta xz, \quad \dot{z} = -kx - az + \frac{k\lambda}{d}. \tag{10}$$

Doing the change of variables in (7) system (10) can be written as

$$\dot{x} = -x - a_1 z - xz, \quad \dot{z} = -x - a_2 z, \tag{11}$$

where $a_1 = \beta k \lambda / d^3$ and $a_2 = a/d$ and again we have renamed (X, Z) as (x, z), and the dot means derivative with respect to the new time T.

Systems (8) and (11) are the same and so their global phase portraits are exactly the same. In short, taking into account the results of this subsection we have proved Theorem 3.

4. Proof of Theorem 4

In this section we describe the α– and the ω–limit sets of all orbits of system (1) contained in B and outside the invariant planes $F_1 = 0$ and $F_2 = 0$.

In section 3 we proved that $I_d(x, y, z, t) = F_i(x, y, z)e^{dt}$ is an invariant of system (1) when $a = d \neq 0$ if $i = 1$ and $\mu = d \neq 0$ if $i = 2$. Let

$$\gamma(t) = \{(x(t), y(t), z(t)) : t \in \mathbb{R}\}$$

be an orbit of the compactified system (1) outside the planes $F_i = 0$ for $i = 1, 2$. Therefore

$$I_d(t, x(t), y(t), z(t)) = h.$$

with $h \in \mathbb{R} \setminus \{0\}$. So

$$F_i(x(t), y(t), z(t))\ e^{dt} = h, \quad \text{for all } t \in \mathbb{R},\ i = \{1, 2\}. \tag{12}$$

Taking the limit in (12) when $t \to -\infty$, we obtain that

$$\lim_{t\to\infty} F_i(x(t), y(t), z(t)) = \pm\infty.$$

Therefore the α–limit is contained in the boundary of the plane $F_i = 0$ at infinity. Then from Figure 1 these α-limit sets can only be one of the four singular points contained in the boundary of $F_i = 0$ at infinity, i.e., q, q', E_2 and E_2' (see Figure 7). So, statement (a) is proved. Now taking the limit in (12) when $t \to \infty$, we obtain that

$$\lim_{t\to\infty} F_i(x(t), y(t), z(t)) = 0.$$

Therefore the ω–limit is contained in the closed plane $F_i = 0$ in the Poincaré ball. To complete the study of the ω-limit sets we first study the finite singular points in $\mathbb{R}^3$ whenever either $d = a$, or $d = \mu$. Since the study is the same we will focus in the case in which $d = a$. We consider different cases.

Case 1: $\lambda = \mu = 0$. In this case the singular points are located at $x = y = 0$. Computing the eigenvalues of the Jacobian matrix at the points of this line, we get that they are 0, $-a$ and $-a - z\beta$. It follows from the normal hyperbolicity theory (see again [4]) that if $-a - z_0\beta < 0$ then the singular point $(0, 0, z_0)$ has a 2-dimensional stable manifold, whereas if $-a - z_0\beta > 0$ then the singular point $(0, 0, z_0)$ has a 1-dimensional stable manifold and 1-dimensional unstable invariant manifold.

Case 2*:* $\mu = 0$ *and* $\lambda \neq 0$. In this case the unique singular point is $(\lambda/a, 0, 0)$. Computing the eigenvalues of the Jacobian matrix at this point we get

$$-a, \qquad \frac{-a^2 \pm \sqrt{a^4 + 4ak\beta\lambda}}{2a}.$$

Since $ak\beta\lambda > 0$ we get that the singular point $(\lambda/a, 0, 0)$ has a 2-dimensional stable manifold and 1-dimensional unstable manifold.

Case 3*:* $\mu = k\beta\lambda/a^2$. In this case the unique singular point is again $(\lambda/a, 0, 0)$. Computing the eigenvalues of the Jacobian matrix at this point we obtain

$$0, \quad -a, \quad -\frac{a^3 + k\beta\lambda}{a^2}$$

So by the normal hyperbolicity theory the singular point $(\lambda/a, 0, 0)$ has either a 2-dimensional stable manifold.

Case 4*:* $\mu \neq k\beta\lambda/a^2$. In this case there are two singular points which are given in (5) (p_0 and p_1). Computing the eigenvalues of the Jacobian matrix at these singular points we get

$$-a, \quad -\frac{a(a+\mu) \pm \sqrt{(a^2 + a\mu)^2 - 4a(a^2\mu - k\beta\lambda)}}{2a}$$

for p_0, and

$$-a, \quad -\frac{a\mu^2 + k\beta\lambda \pm \sqrt{(a\mu^2 + k\beta\lambda)^2 + 4au^2(a^2\mu - k\beta\lambda)}}{2a\mu}$$

for p_1. So, p_0 has a 2-dimensional stable manifold and 1-dimensional unstable manifold when $a^2\mu - k\beta\lambda < 0$, and a 3-dimensional stable manifold when $a^2\mu - k\beta\lambda > 0$. On the other hand, p_1 has a 3-dimensional stable manifold when $a^2\mu - k\beta\lambda < 0$, and a 2-dimensional stable manifold and 1-dimensional unstable manifold when $a^2\mu - k\beta\lambda > 0$.

Now we can finish the proof of statement (b) of Theorem 4. Indeed, the first assertion in statement (b) of Theorem 4 follows directly from Case 1 and Figure 7 whereas the second assertion in statement (b) of Theorem 4 follows directly from Case 2 and Figure 7. Moreover, the third and four assertions in statement (b) of Theorem 4 follow from Cases 3 and 4 and Figure 7.

Acknowledgements

The first author is partially supported by FAPEMIG Grants APQ-01086-15 and APQ-01158-17. The second author is partially supported by the Ministerio de Economía, Industria y Competitividad, Agencia Estatal de Investigación grant MTM2016-77278-P (FEDER), the Agència de Gestió d'Ajuts Universitaris i de Recerca grant 2017 SGR 1617, and the European project Dynamics-H2020-MSCA-RISE-2017-777911. The third author is partially supported by FCT/Portugal through UID/MAT/04459/2013.

References

[1] J. Alavez-Ramírez, G. Blé, V. Castellanos and J. Llibre, *On the global flow of a 3-dimensional Lotka–Volterra system*, Nonlinear Anal. **75** (2012), 4114–4125.

[2] A. Cima and J. Llibre, *Bounded polynomial vector fields*, Trans. Amer. Math. Soc. **318** (1990), 557–579.

[3] F. Dumortier, J. Llibre and J.C. Artés, *Qualitative Theory of Planar Differential Systems*, Springer Verlag, New York, 2006.

[4] H.W. Hirsch, C.C. Pugh and M. Shub, *Invariant manfifolds*, Lecture Notes in Math. **583**, Springer Verlag, Berlin, 1977.

[5] P. De Leenheer and H.L. Smith, *Virus dynamics: a global analysis*, SIAM J. Appl. Math. **63** (2003), 1313–1327.

[6] J. Llibre, M. Messias and A.C. Reinol, *Quadratic polynomial differential systems in $\mathbb{R}^3$ having invariant planes with total multiplicity* 9, Rendiconti del Circolo Matematico di Palermo **67** (2018), 569–580.

[7] R.M. May and M.A. Nowak, *Virus Dynamics. Mathematical Principles of Immunology and Virology*, Oxford University Press, New York, 2000.

[8] L. Min, Y. Su and Y. Kuang, *Mathematical analysis of a basic virus infection model with application to HBV infection*, Rocky Mount. J. Math. **38** (2008), 1–13.

[9] C. Valls, *Invariant algebraic surfaces fo a virus dynamics*, Z. Angew. Math. Phys. **66** (2015), 1315–1328.

[1]Instituto de Matemática e Computação, Universidade Federal de Itajubá, Avenida BPS 1303, Pinheirinho, CEP 37.500–903, Itajubá, MG, Brazil.

E-mail address: scalco@unifei.edu.br

[2]Departament de Matemàtiques, Universitat Autònoma de Barcelona, 08193 Bellaterra, Barcelona, Spain.

E-mail address: jllibre@mat.uab.cat

[3]Departamento de Matemàtica, Instituto Superior Técnico, Universidade de Lisboa, 1049-001 Lisboa, Portugal.

E-mail address: cvalls@math.ist.utl.pt